Croatian Society for Materials Protection

Metalurgija/Metallurgy

Vol. 66 No. 1 / 2027

Corrosion Resistance of ALD Al_2O_3 Coatings on 310S Stainless Steel for Fencing Applications in Tropical Forest Environments

Li Zhan[1,*] and Yanli Jiang[1]

https://doi.org/10.64486/m.66.1.5

[1] Harbin University, Harbin City, No. 109 Zhongxing Avenue, Nangang District, Heilongjiang Province, China, 150086; jylzhl@163.com
* Correspondence: zhanli@hrbu.edu.cn

Type of the Paper: Article
Received: March 9, 2026
Accepted: May 17, 2026

Abstract: This study investigates the corrosion protection of 310S stainless steel by Al_2O_3 coatings prepared using an ozone-assisted atomic layer deposition (ALD) process. A dense and uniform Al_2O_3 coating with a thickness of approximately 150 nm was deposited on the steel surface. The coating morphology, phase composition, adhesion, high-temperature oxidation resistance, and corrosion behavior were evaluated using SEM/EDS, AFM, XRD, Vickers indentation, immersion tests, and electrochemical measurements. The results show that the ALD Al_2O_3 coating effectively covers surface defects, exhibits good adhesion to the substrate, and significantly improves corrosion resistance in chloride-containing and acidic media. The coated sample also maintains structural integrity after oxidation at 800 °C, indicating improved high-temperature stability and reduced chromium outward diffusion. These results demonstrate that ozone-assisted ALD Al_2O_3 coating is a promising surface protection method for 310S stainless steel used in outdoor fencing and ecological protection applications.

Keywords: outdoor fencing; 310S stainless steel; Al_2O_3 coating; atomic layer deposition; corrosion resistance

1. Introduction

Outdoor fencing is an important infrastructure for ecological protection, forestry management, and wildlife habitat conservation. During long-term service in tropical and subtropical forest and mountainous environments, fencing systems are exposed to severe corrosion conditions [1]. The outdoor environment is characterized by long-term high humidity, rain, dew, and soil salts, which maintain the fencing steel in a persistently wet state. Meanwhile, humic acid from forest humus decomposition and acid rain from industrial emissions make the surrounding corrosive media weakly acidic; hydrogen ions and sulfate ions in the media accelerate the uniform corrosion of stainless steel and cause dissolution and damage to the passive film [4], [5].

The field environment has a significant diurnal temperature difference: the surface temperature of fencing steel can exceed 60℃ in summer, and even faces short-term high-temperature burning under extreme conditions. This high-temperature environment not only accelerates corrosion, but also promotes the outward diffusion of Cr in stainless steel, which is converted into volatile and highly toxic Cr^{6+} compounds, causing irreversible heavy metal pollution to forest soil, water bodies, and organisms [6], [7]. In addition, outdoor fencing is mostly laid in large outdoor areas with high maintenance difficulty and cost, which requires the protective

coating to have long-term service stability, strong adhesion, uniform protective performance, and excellent adaptability to the complex geometric structure of the fencing.

310S stainless steel is a low-carbon, high-Cr, high-Ni austenitic stainless steel with excellent initial corrosion resistance, high-temperature oxidation resistance, and mechanical strength. Compared with ordinary carbon steel and 304/316 stainless steel, it is more suitable for the long-cycle service requirements of outdoor fencing and has been widely used in forestry protection engineering in recent years [8]. However, long-term field service results show that 310S stainless steel still suffers from passive film breakdown, pitting propagation, and accelerated uniform corrosion in Cl^--containing forest soil and acid rain. Meanwhile, outward Cr diffusion and Cr^{6+} formation at high temperatures will not only weaken the oxidation resistance of the steel itself, but also violate the core demand of ecological protection, which severely restricts the long-term application of 310S stainless steel in outdoor fencing engineering. Therefore, developing a surface protection process for 310S stainless steel that adapts to outdoor fencing service scenarios, with both high-efficiency anti-corrosion and environmentally friendly Cr-blocking performance, has become an urgent technical problem in forestry engineering and material protection fields.

Modifying metal surface properties via coating technology is the core method to improve the corrosion resistance and high-temperature protection performance of stainless steel, and related technologies have been widely studied in chemical, energy, and marine engineering fields [9]. Among numerous protective coating systems, Al_2O_3 coating is an ideal choice for long-term stainless steel protection due to its excellent chemical stability, high-temperature inertia, corrosion resistance, and high hardness. It can not only act as a physical barrier to isolate corrosive media from the metal substrate, but also form a stable corundum phase at high temperatures, effectively hindering inward oxygen diffusion and outward chromium diffusion, thus avoiding the formation and release of toxic Cr^{6+} [10], [11].

At present, conventional preparation methods for Al_2O_3 coatings on stainless steel include thermal spraying, magnetron sputtering, chemical vapor deposition (CVD), sol-gel, and electrophoretic deposition. However, these methods have significant technical limitations: thermal spraying and CVD require high deposition temperatures, which easily damage the mechanical properties of the stainless steel substrate; magnetron sputtering and sol-gel methods are difficult to prepare uniform and dense coatings on complex-shaped substrates, with poor step coverage; coatings prepared by electrophoretic deposition have weak adhesion and high porosity, which are prone to peeling and protection failure during long-term field service [12], [13]. For complex structural parts such as grid-like, special-shaped cross-section outdoor fencing, conventional coating processes cannot achieve full-surface uniform protection, and local corrosion is very likely to occur at coating defects, eventually leading to overall failure of the fencing.

Atomic Layer Deposition (ALD) is a thin film preparation technology based on periodic self-limiting reactions of gas-phase precursors, which can deposit materials on the substrate surface layer by layer in the form of monoatomic films [14]. Compared with conventional coating methods, ALD has three core advantages: first, precise thickness control at the sub-nanometer level, with a uniform hundred-nanometer coating prepared by 1000 deposition cycles; second, excellent conformality and uniformity, enabling full-coverage deposition on complex-shaped and porous substrates, perfectly adapting to the grid structure of outdoor fencing; third, low deposition temperature, high coating density, and strong substrate adhesion, allowing the preparation of pinhole-free amorphous Al_2O_3 coatings at low temperatures without damaging the stainless steel substrate.

In recent years, research on ALD Al_2O_3 coatings for stainless steel corrosion protection has increased. Domestic and foreign scholars have confirmed that ALD Al_2O_3 coatings can significantly improve the corrosion resistance of 316L and 304 stainless steel in chloride-containing and acidic media [15], [16], [17]. Related studies have also verified that surface hydroxylation pretreatment can effectively enhance the interfacial adhesion between ALD Al_2O_3 coatings and stainless steel substrates [18], [19]. However, there is still a gap in the special research on 310S stainless steel for outdoor fencing applications, especially systematic studies that simultaneously consider field environment corrosion resistance, high-temperature Cr-blocking eco-friendliness, and

https://doi.org/10.64486/m.66.1.5

complex structure adaptability have not been reported. In addition, most existing studies focus on the application of ALD technology in microelectronics and precision devices, and its application potential in outdoor large-scale engineering component protection still needs to be systematically explored [20].

Aiming at the corrosion failure risk of 310S stainless steel for outdoor fencing and the industry pain point that existing coating processes cannot adapt to the complex geometric structure of fencing and achieve long-term uniform protection, this study adopts an improved ALD technology to prepare high-quality Al_2O_3 protective coatings on 310S stainless steel through an ozone pre-injection process. The microstructure, phase composition, elemental chemical state, and substrate bonding performance of the ALD Al_2O_3 coating are systematically studied. Meanwhile, the corrosion resistance behavior and protective mechanism of the coating in typical corrosive environments are revealed through immersion tests simulating outdoor corrosive media. This study verifies the applicability of the process in complex outdoor corrosive environments and provides a high-precision, full-coverage, and long-term stable surface protection scheme for 310S stainless steel used in outdoor fencing applications.

2. Materials and Methods

2.1. Experimental Materials and Substrate Pretreatment

Commercial 310S austenitic stainless steel was used as the substrate material, and its main chemical composition is shown in Table 1. Before Al_2O_3 coating deposition, substrate pretreatment was performed to remove surface contaminants and natural passive film, improve coating adhesion and film-forming uniformity, and construct hydroxyl active sites on the substrate surface to enhance the chemical bonding of the Al_2O_3 film and the reaction activity during deposition.

Table 1. Chemical composition of 310S stainless steel

Stainless Steel	C/%	Si/%	Mn/%	P/%	S/%	Cr/%	Ni/%
310S	0.05	0.54	0.92	0.025	0.001	25.72	19.49

The substrate pretreatment process was as follows: 1.5 mm thick 310S stainless steel plates were cut into 15 mm × 15 mm × 1.5 mm block samples by a wire cutting machine; the sample surfaces were ground step by step with 120#, 240#, 400#, 600#, 800# metallographic sandpapers, and then mechanically polished by a metallographic grinding and polishing machine to simulate the surface treatment process in actual outdoor fencing production; the polished samples were ultrasonically cleaned in deionized water and anhydrous ethanol for 15 min each to remove surface oil and abrasive debris; after cleaning, the samples were stored in a vacuum drying oven at constant temperature for later use.

2.2. Preparation of Al_2O_3 Coating

The Al_2O_3 coating was prepared by an improved ALD technology, with the core innovation of pulse-injected ozone to provide sufficient hydroxyl active sites on the substrate surface before each deposition cycle, so as to improve precursor reaction efficiency and film-forming quality. The deposition process was carried out in an ALD chamber at 150 ℃, with the chamber pressure controlled at (10–100) mbar. Trimethylaluminum (TMA) and deionized water were used as dual precursors, and nitrogen was used as carrier gas and purge gas.

The process parameters of a single deposition cycle were as follows:

- Ozone pre-injection: O_3 was injected in pulse with a flow rate of (50–200) sccm. After pressure holding for 20–30 s, high-purity N_2 was introduced for purging for 25 s to construct hydroxyl active sites on the substrate surface.
- TMA pulse: TMA was injected in pulse for 0.02 s with a flow rate of (1~10) sccm. After pressure holding for 8 s, high-purity N_2 was used for purging for 25 s to enable saturated self-limiting reaction between TMA and hydroxyl groups on the substrate surface.

https://doi.org/10.64486/m.66.1.5

- H_2O pulse: Deionized water was injected in pulse for 0.1 s with a flow rate of (1–10) sccm. After pressure holding for 8 s, high-purity N_2 was used for purging for 25 s to enable reaction between H_2O and surface-adsorbed TMA to generate a monoatomic Al_2O_3 layer.

The above deposition cycle was repeated 1000 times to obtain the final ALD Al_2O_3 coated 310S stainless steel sample.

2.3. Microstructure Characterization

A JSM-6510 scanning electron microscope (SEM) was used to observe the surface and cross-sectional morphology of the 310S substrate and coated samples, and the element distribution was analyzed with a supporting energy dispersive spectrometer (EDS). A Vickers hardness tester was used to test the coating adhesion via Vickers indentation experiments under HV0.1 and HV0.3 loads. Al_2O_3 coating prepared by electrophoretic deposition under the same process parameters was used as the control, and the adhesion between the coating and the substrate was evaluated by the deformation and cracking of the coating around the indentation.

The phase composition of the samples was characterized by X-ray diffraction (XRD) with a diffraction angle range of 20°–80°, and phase analysis was performed using Jade 6 software.

2.4. Performance Test Methods

A SJG-12 muffle furnace was used to conduct isothermal oxidation tests on 310S substrate and coated samples in an air atmosphere at 800 ℃ to simulate extreme high-temperature and burning scenarios in outdoor environments. After reaching the set time, the samples were cooled to room temperature with the furnace, and the mass of the samples before and after oxidation was weighed with a high-precision electronic balance. The oxidized samples were characterized to analyze surface morphology and phase evolution.

To verify the long-term corrosion resistance of the coating and simulate the corrosion environment of outdoor fencing in wet soil and rainwater, the 310S substrate and coated samples were immersed in 3.5 wt.% NaCl solution for 10 h and 0.1 mol/L H_2SO_4 solution for 4 h, respectively. The surface morphology after corrosion was observed, and the corrosion products and surface element content changes were analyzed.

3. Results and Discussion

3.1. Microstructure and Surface Characteristics of ALD Al_2O_3 Coating

3.1.1. Surface Morphology and Thickness Analysis

310S stainless steel is mainly composed of austenite phase with a face-centered cubic (FCC) crystal structure. The surface morphology of the 310S substrate and 310S-ALD Al_2O_3 coated sample is shown in Figure 1. It can be seen from Figure 1 (a) and (b) that there are micro-defects such as a small number of pores on the 310S substrate surface, while the surface of the ALD Al_2O_3 coated sample is uniform and smooth, forming a dense oxide film.

From Figure 1 (c) and (d), both the 310S substrate and coated sample show strip scratches caused by grinding and polishing. However, the substrate surface still has obvious defects, while the coated sample surface is smooth as a whole, with substrate defects effectively covered. This reflects the dense and uniform characteristics of the ALD Al_2O_3 coating, as well as the excellent conformal coverage of ALD technology, which can perfectly adapt to the steel surface with micro-defects after grinding for outdoor fencing applications and avoid corrosion initiation at the defects.

https://doi.org/10.64486/m.66.1.5

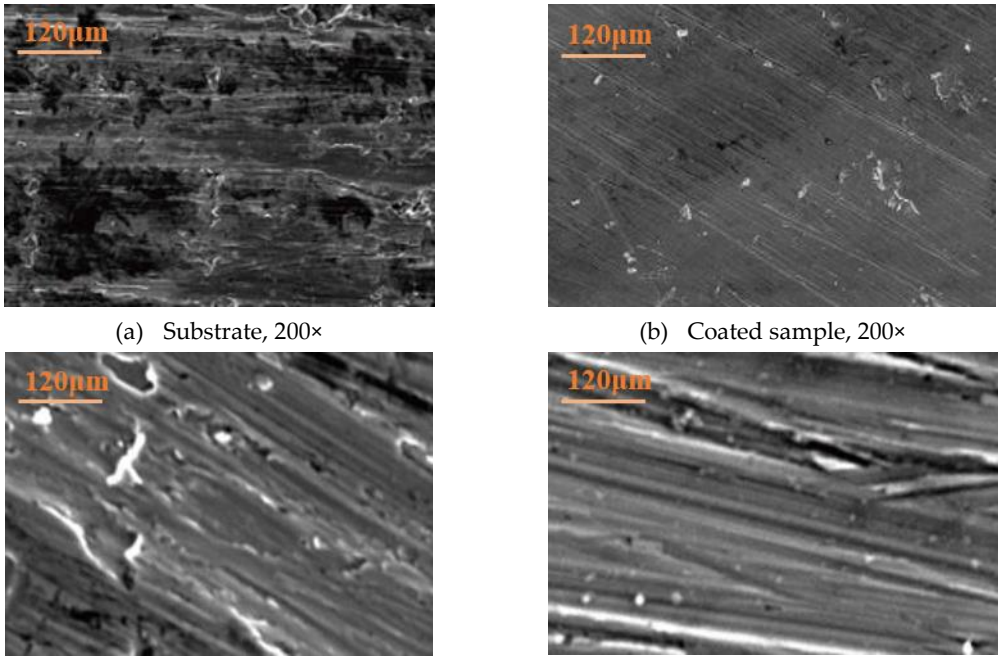

(a) Substrate, 200× (b) Coated sample, 200×

(c) Substrate, 3000× (d) Coated sample, 3000×

Figure 1. Surface morphology of 310S substrate and ALD Al_2O_3 coated sample

The Cu-plated 310S stainless steel samples with atomic layer deposition (ALD) Al_2O_3 coating were treated by cold mounting, ground and polished until the cross-section was fully exposed, followed by SEM-EDS line scan analysis. The results are shown in Figure 2. It can be seen from Figure 2 that the characteristic elements in the left substrate region are Fe, Cr and Ni, the characteristic element in the right Cu-plated layer is Cu, while Al and Cu are the dominant elements at the interface between the substrate and the Cu-plated layer, confirming that the gray-white film at the interface is the Al_2O_3 coating.

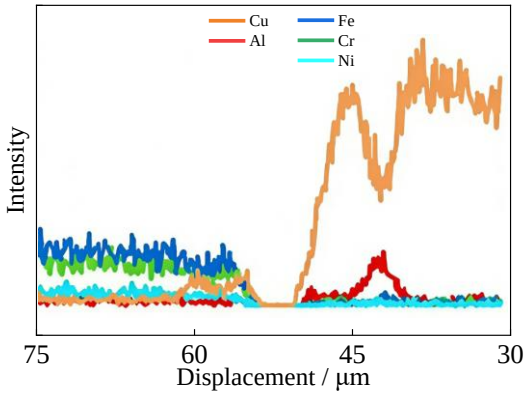

Figure 2. SEM-EDS line scan result of the interface between the substrate and the ALD Al_2O_3 coating

In addition, the fabrication of ALD Al_2O_3 coating requires repeated unit deposition cycles, and the precise control of the Al_2O_3 coating thickness is achieved through layer-by-layer deposition. After 1000 deposition cycles, a uniform and dense nano-Al_2O_3 coating with the designed thickness can be formed on the surface of 310S stainless steel substrate. The two-dimensional (2D) atomic force microscopy (AFM) characterization result of the interface between the 310S substrate and the ALD Al_2O_3 coating is shown in Figure 3. It can be seen that the Al_2O_3 film prepared by ALD has a dense structure, and the coating thickness at the interface is about 150 nm.

https://doi.org/10.64486/m.66.1.5

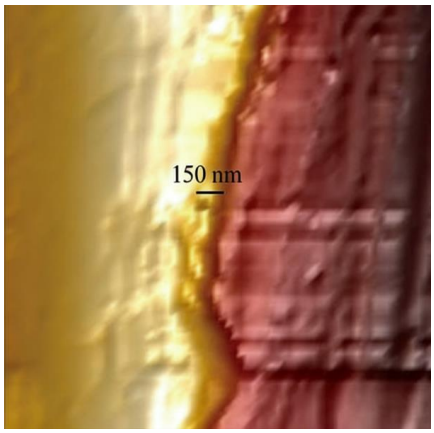

Figure 3. 2D AFM image of the interface between the substrate and the ALD Al_2O_3 coating

3.1.2 Phase Composition Analysis

The XRD patterns of the 310S substrate and ALD Al_2O_3 coated sample are shown in Figure 4. In the diffraction angle range of 20°–80°, both the substrate and coated sample have 3 distinct diffraction peaks at the same positions. Analyzed by Jade 6 software, these peaks are all characteristic peaks of austenite, indicating that the 310S steel is composed of single-phase austenite, with FeCr(Ni) as the matrix phase.

For the ALD Al_2O_3 coated sample before oxidation, there are no other crystalline peaks representing the film except the substrate peak of FeCr(Ni), which mainly shows a broad diffuse peak (e.g., at 75°), consistent with the characteristics of amorphous alumina. This is because the Al_2O_3 film deposited at 150 ℃ is amorphous, and crystalline structure can only be formed at 400 ℃ and above. XRD detects the periodic lattice arrangement inside the material and generates diffraction peaks through Bragg diffraction. However, the atomic arrangement of amorphous alumina has no long-range order, only short-range order, so it will not form clear Bragg diffraction peaks. In addition, the low content of alumina deposited by ALD is another reason for the absence of obvious crystalline diffraction peaks.

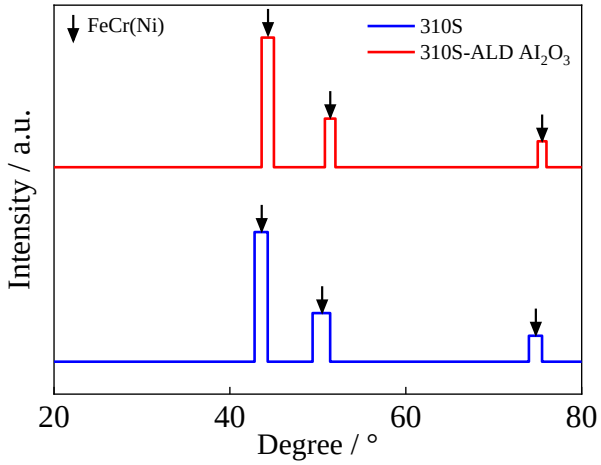

Figure 4. XRD patterns of 310S substrate and ALD Al_2O_3 coated sample

3.1.3 Electrochemical Impedance Spectroscopy Analysis

Electrochemical Impedance Spectroscopy (EIS) is a classic method for evaluating the corrosion resistance of metallic materials. The Nyquist plots of the 310S substrate and the ALD Al_2O_3 coated sample are shown in Figure 5. Generally, the larger the diameter of the capacitive arc in the Nyquist plot, the better the corrosion resistance of the material. It can be seen from Figure 5 that the 310S substrate has a small capacitive arc diameter, while the ALD Al_2O_3 coated sample has a significantly increased capacitive arc diameter, indicating that the

https://doi.org/10.64486/m.66.1.5

ALD Al_2O_3 coating can exert a stronger barrier protection effect on the substrate during the electrochemical corrosion process.

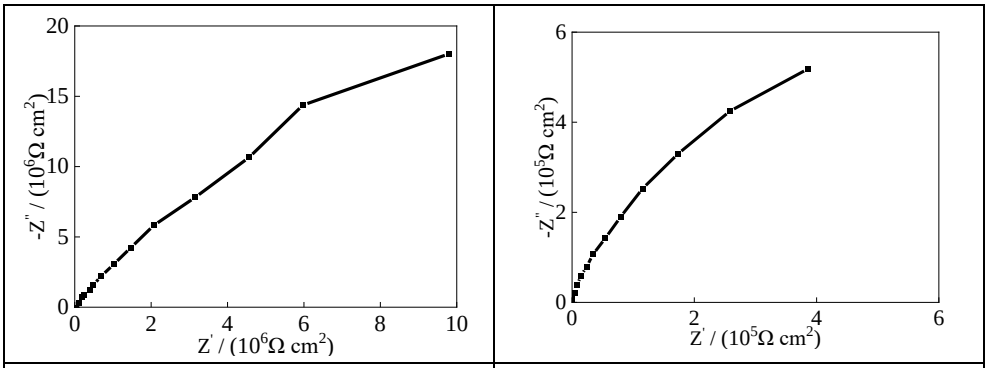

(a) Al_2O_3 coating (b) Substrate

Figure 5. Nyquist curves

The potentiodynamic polarization curves of the 310S substrate and the ALD Al_2O_3 coated sample in 3.5 wt.% NaCl solution and 0.1 mol·L^{-1} H_2SO_4 solution are shown in Figure 6, respectively. It can be seen from Figure 6 that both samples show obvious passivation regions in the two corrosive media. The passivation behavior of the 310S substrate is attributed to the formation of a dense Cr_2O_3 passive film on the substrate surface in the oxidative corrosive environment, which can inhibit the further corrosion of the substrate.

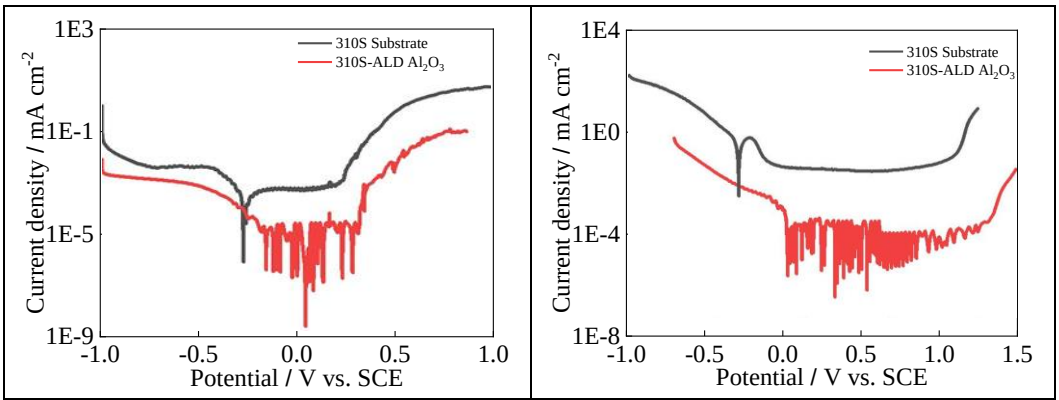

(a) 3.5 wt.% NaCl solution (b) 0.1 mol·L^{-1} H_2SO_4 solution

Figure 6. Polarization curves

In this study, based on the interfacial reaction characteristics reflected by the EIS test results, equivalent circuits with single time constant and dual time constants were used to fit the impedance data of the 310S substrate and the ALD Al_2O_3 coating, respectively. Among them, the R(QR) equivalent circuit was adopted for the 310S substrate, and the R(Q(R(QR))) equivalent circuit was adopted for the ALD Al_2O_3 coated sample. The fitting results of the EIS test data are shown in Table 2. It can be seen from Table 2 that the CPEdl value of the ALD Al_2O_3 coated sample is lower than the CPEc value, indicating that the ALD Al_2O_3 coating has excellent corrosion resistance.

Table 2. EIS test results

Stainless Steel	R_s/Ω·cm^2	n_1	R_c/Ω·cm^2	n_2	R_{ct}/Ω·cm^2	CPE_cY_0 ($\Omega^{-1}cm^{-2}$ $s^a)^n$	$CPE_{dl}Y_0$ ($\Omega^{-1}cm^{-2}$ $s^a)^n$
Substrate	42.40	0.80			$1.54*10^5$		$1.20*10^{-5}$
ALD coating	7.12	0.77	$4.22*10^4$	0.8	$1.04*10^6$	$2.76*10^{-7}$	$1.43*10^{-7}$

https://doi.org/10.64486/m.66.1.5

3.1.4. Interfacial Adhesion Performance of the Coating

To evaluate the adhesion of the ALD Al_2O_3 coating, Vickers indentation tests were carried out on the coating samples prepared by electrophoretic deposition and ALD technology respectively. Figure 7 (a) and (c) are SEM images of Vickers indentations on the surface of the electrophoretic deposition coating under different loads. It can be seen that the deformation area of the electrophoretic coating surface under pressure is large and irregular. With the increase of load, the deformation area and deformation degree increase significantly, indicating weak adhesion between the coating and the substrate.

Figure 7 (b) and (d) are SEM images of Vickers indentations on the surface of the ALD prepared coating under different loads. The deformation area on the ALD Al_2O_3 coated sample surface is relatively regular, with small size change and no obvious cracks. Under pressure, the ALD Al_2O_3 coating can disperse stress uniformly to a certain extent, realizing cooperative deformation between the substrate and the coating.

Compared with the conventional electrophoretic deposition coating, the ALD Al_2O_3 coated sample has a more regular and smaller deformation area under pressure, which further proves the excellent adhesion of the ALD Al_2O_3 coating. This excellent adhesion is attributed to the self-limiting growth mode of ALD, which can control film growth at the atomic level, thus forming a continuous, uniform and highly adherent coating on the substrate.

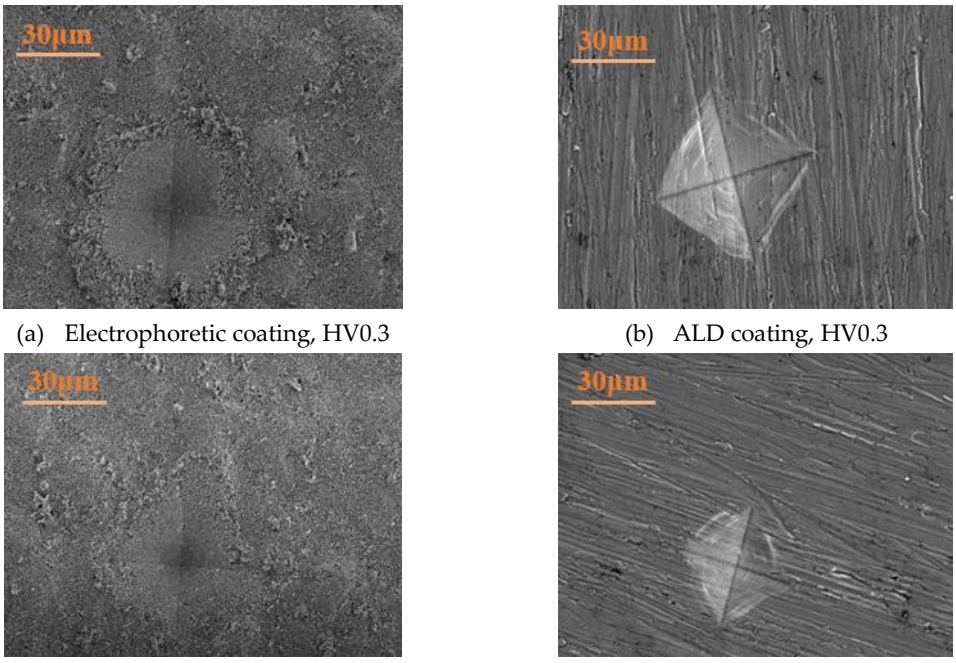

(a) Electrophoretic coating, HV0.3 (b) ALD coating, HV0.3

(C) Electrophoretic coating, HV0.1 (D) ALD coating, HV0.1

Figure 7. SEM images of Vickers indentations on the coating surface

3.2. High-Temperature Oxidation and Cr-Blocking Performance

The surface morphology of the samples after high-temperature oxidation is shown in Figure 8. After high-temperature oxidation, the microstructure of the 310S-ALD Al_2O_3 coated sample is significantly different from that of the 310S substrate. With the increase of oxidation time, the oxide film on the surface of the ALD Al_2O_3 coated sample still maintains good compactness, showing more excellent high-temperature oxidation resistance. After isothermal oxidation in high-temperature air for 10 h and 30 h respectively, the oxide film on the coated sample surface remains continuous and uniform, with almost no cracks and peeling.

This indicates that the ALD Al_2O_3 coating can maintain structural compactness and integrity for a long time in the environment simulating extreme high temperature and short-term burning in outdoor environments, and effectively hinder the outward diffusion of Cr element in the substrate, realizing the coordination of material protection and ecological environment protection.

https://doi.org/10.64486/m.66.1.5

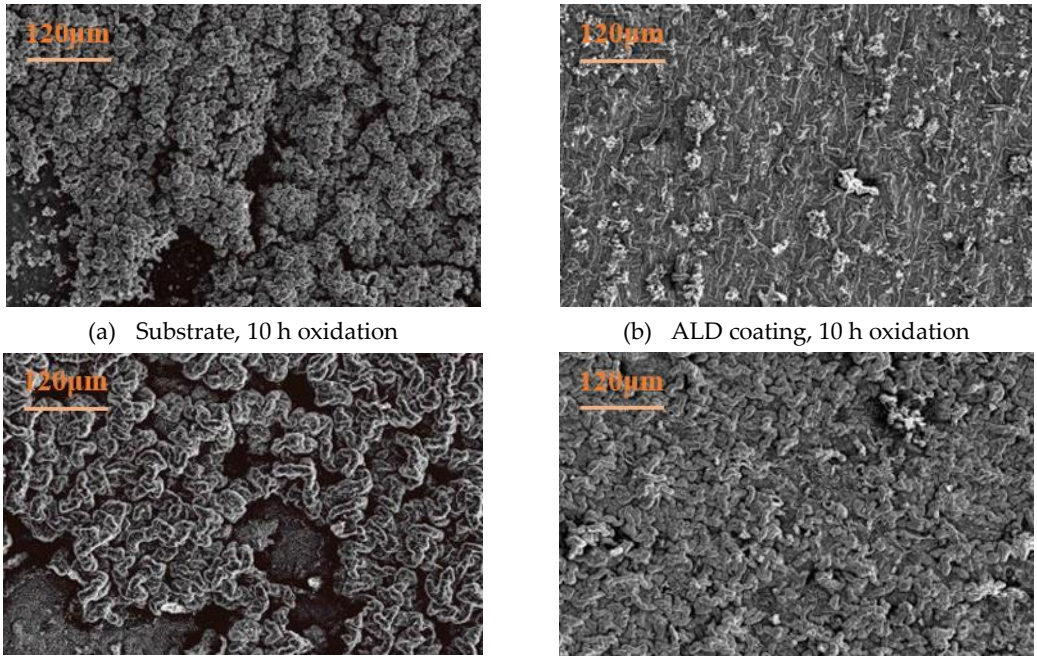

(a) Substrate, 10 h oxidation (b) ALD coating, 10 h oxidation

(c) Substrate, 30 h oxidation (d) ALD coating, 30 h oxidation

Figure 8. SEM images of 310S substrate and ALD Al_2O_3 coated sample after isothermal oxidation for different durations

3.3. Corrosion Resistance and Protective Mechanism

3.3.1. Corrosion Morphology and Corrosion Products

To further observe the long-term corrosion behavior of the 310S substrate and ALD Al_2O_3 coated sample in corrosive media, immersion experiments were carried out. Figure 9 shows the 100× magnification SEM images of the 310S substrate and coated sample after immersion in 3.5 wt.% NaCl solution and 0.1 mol/L H_2SO_4 solution for set durations.

It can be seen from Figure 9 (a) and (b) that there are fine strip scratches on the 310S substrate surface caused by grinding and polishing, while the surface of the ALD Al_2O_3 coated sample is relatively smooth, with scratches effectively covered by the Al_2O_3 coating. Chloride ions have strong penetrating power and are easy to damage the passive film on the 310S stainless steel surface; once the passive film is locally damaged, the exposed substrate will undergo electrochemical reaction with sodium chloride solution, causing local corrosion such as pitting. As shown in Figure 5 (c), after immersion in 3.5 wt.% NaCl solution, slight pitting occurs on the 310S substrate surface, with local depressions or fine holes; with the extension of corrosion time, the corrosion on the substrate surface is intensified, the pitting pits are deepened, local pitting aggregation areas appear, and the number of holes increases. The nickel element in 310S stainless steel can improve its corrosion resistance in sulfuric acid. When the concentration of dilute sulfuric acid is low, the passive film on its surface can resist corrosion to a certain extent. However, SO_4^{2-} has strong oxidizing and corrosive properties, which can destroy the Cr_2O_3 passive film and expose the metal matrix to the acid to induce corrosion. As shown in Figure 5 (e), in 0.1 mol/L H_2SO_4 solution, the passive film on the 310S substrate surface is seriously damaged, accompanied by micro pits and slight holes; with the extension of corrosion time, uniform corrosion is intensified, and obvious pit propagation occurs on the substrate surface. As shown in Figure 9 (d) and (f), no obvious pitting is observed on the surface of the ALD Al_2O_3 coated sample in both 3.5 wt.% NaCl solution and 0.1 mol/L H_2SO_4 solution, and the coating maintains good integrity with excellent protective effect. The corrosion duration was further extended, with 48 h of corrosion in 3.5 wt.% NaCl solution and 24 h of corrosion in 0.1 mol·L^{-1} H_2SO_4 solution, respectively. The results are shown in Figure 9 (g) and (h). The above results indicate that compared with the 310S substrate, the ALD Al_2O_3 coated sample has significantly improved uniform corrosion resistance and localized corrosion resistance after immersion in the two corrosive media.

https://doi.org/10.64486/m.66.1.5

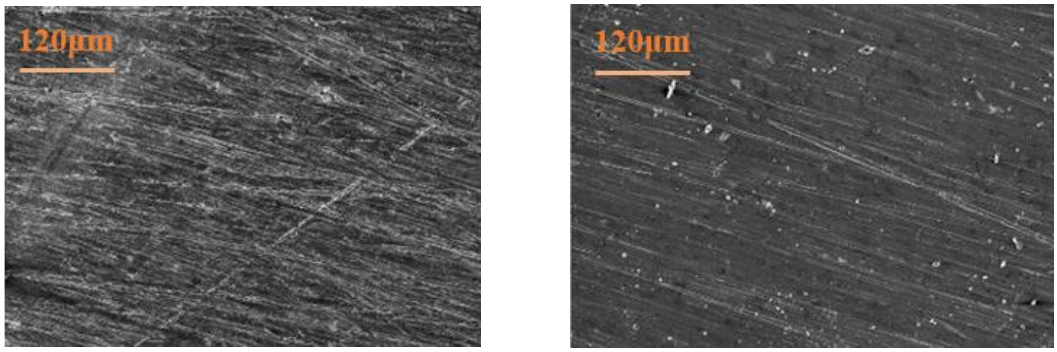

(a) Uncorroded substrate (b) Uncorroded ALD coating

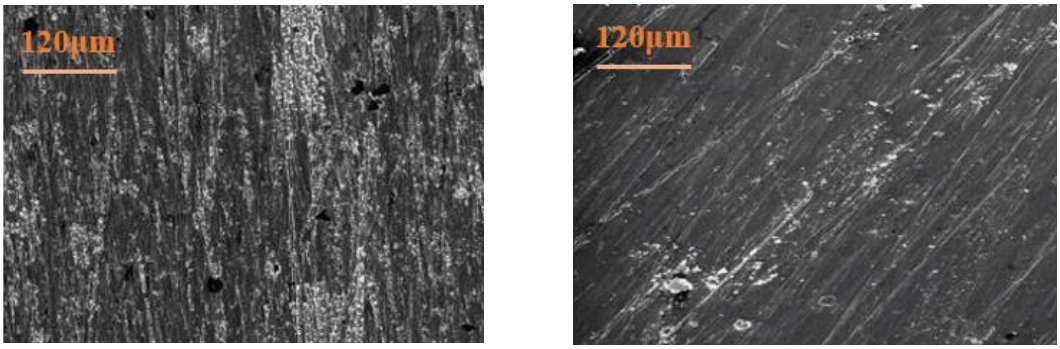

(c) Substrate, 10 h immersion in NaCl solution (d) ALD coating, 10 h immersion in NaCl solution

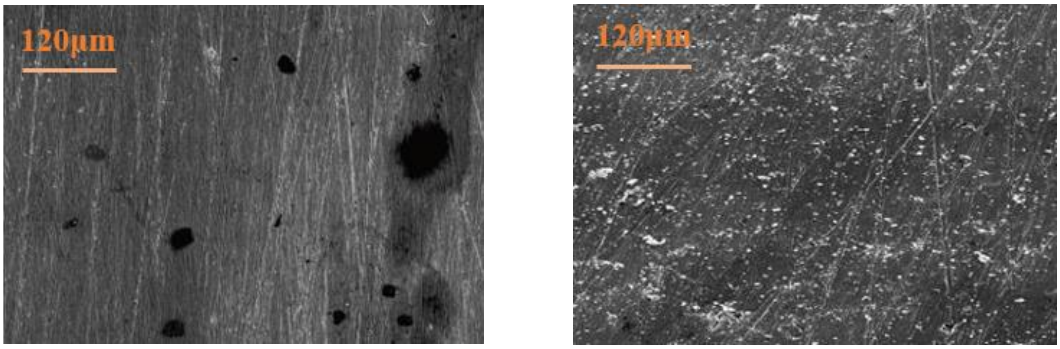

(e) Substrate, 4 h immersion in H_2SO_4 solution (f) ALD coating, 4 h immersion in H_2SO_4 solution

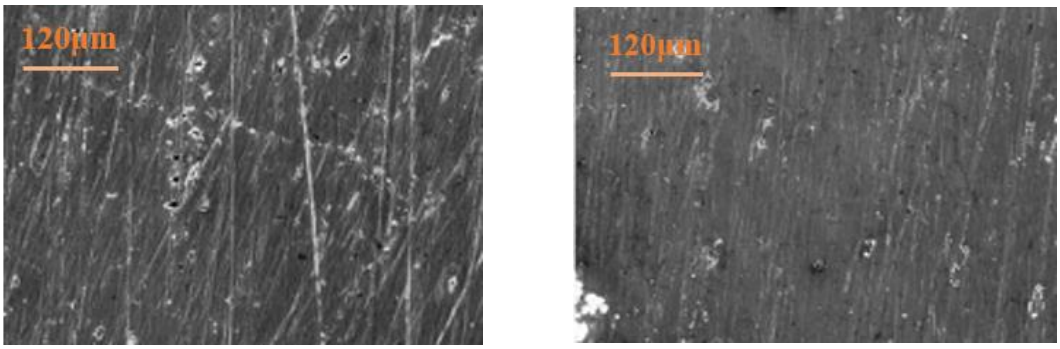

(g) ALD coating, 24 h immersion in H_2SO_4 solution (h) ALD coating, 48 h immersion in NaCl solution

Figure 9. SEM images of samples after immersion corrosion

https://doi.org/10.64486/m.66.1.5

The corrosion protection effect of the Al_2O_3 coating on 310S stainless steel is realized through the synergy of multiple mechanisms, forming an efficient and stable protection system.

The primary mechanism is the physical barrier effect. The ALD-prepared Al_2O_3 coating has an atomic-level dense structure without obvious pores and cracks, which can effectively block direct contact between corrosive media and the substrate, and significantly reduce the penetration rate of corrosive media. The amorphous structure of the coating further strengthens this effect: amorphous materials have no grain boundary defects, and the diffusion path of corrosive media in the coating is complex and long, which greatly prolongs the time for corrosive media to reach the substrate surface.

The second is the chemical stability mechanism. Al_2O_3 has extremely high chemical inertness, which is not easy to dissolve or react in acidic and neutral corrosive media, and can maintain structural integrity for a long time. Compared with the Cr_2O_3 passive film on 310S stainless steel, Al_2O_3 has stronger chemical stability. Especially in high chloride ion environments, Cr_2O_3 easily combines with chloride ions to form soluble chromium salts, leading to passive film damage, while Al_2O_3 has no obvious chemical reaction with chloride ions and can maintain coating structural stability. At the same time, the Al_2O_3 coating can inhibit the diffusion of chromium in the substrate, reduce the formation of high-valent chromium compounds, lower the toxicity of corrosion products, and achieve eco-friendly protection.

The third is the secondary protection mechanism. In corrosive environments, a slight hydration reaction occurs on the Al_2O_3 coating surface, forming a dense $Al(OH)_3$ secondary protective layer. $Al(OH)_3$ has good chemical stability and adhesion, which can fill the possible micro-defects on the coating surface, further block the penetration channels of corrosive media, and form a dual protective structure of "coating - secondary protective layer". This self-healing protective effect can effectively make up for the possible micro-defects in the coating preparation process, improve the long-term service stability of the coating, and is especially suitable for the complex and changeable corrosion conditions in the outdoor environment.

In outdoor service environments, the above protective mechanisms work together to effectively inhibit all links of the corrosion reaction: the physical barrier blocks the penetration of corrosive media, the chemical stability ensures the structural integrity of the coating, and the secondary protection fills the micro-defects. The three together form a comprehensive protection system against complex factors such as high humidity, high chloride ions, acidic media and mechanical wear, which significantly improves the corrosion resistance and service life of 310S stainless steel.

4. Conclusions

Aiming at the service pain points of 310S stainless steel for outdoor fencing and the limitations of existing protection technologies, this work developed an ozone pre-injection modified ALD process to prepare Al_2O_3 protective coatings, and systematically investigated the microstructure, interfacial bonding performance, extreme environment protection effect and mechanism of the coating. The main conclusions are as follows:

1. The ozone pre-injection modified ALD process can fabricate high-quality amorphous Al_2O_3 coating with a thickness of ~150 nm and a growth rate of 0.15 nm/cycle on 310S stainless steel surface. The low-temperature deposition process at 150 ℃ avoids damage to the microstructure and mechanical properties of the stainless steel substrate. The unique self-limiting reaction mode of ALD endows the coating with atomic-level compactness and excellent conformal coverage, which can fully adapt to the complex grid-like geometric structure of fencing components and micro-defects on the substrate surface. Compared with Al_2O_3 coatings prepared by traditional electrophoretic deposition, the coating has more excellent interfacial bonding strength and cooperative deformation ability with the substrate, with no obvious cracking around the Vickers indentation under HV0.1 and HV0.3 loads.
2. In the environment simulating extreme high-temperature and short-term burning in outdoor environments, the coating can maintain structural compactness and integrity for 30 h of isothermal oxidation, effectively hinder the outward diffusion of Cr element in the substrate, avoid the formation and release of toxic Cr^{6+}, and realize the coordination of material protection and ecological environment protection, which further improves the long-term service stability of the coating in complex field environments.

https://doi.org/10.64486/m.66.1.5

3. Quantitative electrochemical tests and long-term immersion tests simulating outdoor service conditions confirm that the ALD Al_2O_3 coating can significantly improve the comprehensive protective performance of 310S stainless steel. The charge transfer resistance of the coated sample reaches 1.04×10^6 $\Omega\cdot cm^2$, which is significantly higher than that of the bare 310S substrate. In Cl^--containing neutral medium and weakly acidic sulfuric acid medium, the coating can effectively inhibit pitting initiation and uniform corrosion caused by passive film breakdown. After immersion in 3.5 wt.% NaCl solution for 48 h and 0.1 $mol\cdot L^{-1}$ H_2SO_4 solution for 24 h respectively, the coating still maintains its structural integrity, with no obvious pitting corrosion observed on the sample surface.

References

[1] E. Baker and W. Kirk, "Long-Term Atmospheric Corrosion Behavior of Various Grades of Stainless Steel in Rural, Industrial, and Marine Environments," in Corrosion Testing and Evaluation: Silver Anniversary Volume, West Conshohocken, PA, USA: ASTM International, 1990, pp. 177–190. https://doi.org/10.1520/stp39189s

[2] C. G. Kang, S. K. Lee, S. Choe, et al., "Intrinsic Photocurrent Characteristics of Graphene Photodetectors Passivated with Al_2O_3," Optics Express, vol. 21, no. 19, pp. 23391–23396, Sep. 2013. https://doi.org/10.1364/oe.21.023391

[3] V. M. P. Wang, "Chloride-Induced Alterations of the Passive Film on 316L Stainless Steel and Blocking Effect of Pre-Passivation," Electrochimica Acta, vol. 329, p. 135159, Jan. 2020. https://doi.org/10.1016/j.electacta.2019.135159

[4] A. Trentin, A. Mardoukhi, A. Lambai, et al., "Pitting Corrosion of Austenitic and Duplex Stainless Steels in Dilute Acids at Elevated Temperature: Effect of Electrolyte Chemistry and Material Microstructure," Corrosion Science, vol. 247, p. 112769, Mar. 2025. https://doi.org/10.1016/j.corsci.2025.112769

[5] Y. C. Tang, S. Katsuma, S. Fujimoto, et al., "Electrochemical Study of Type 304 and 316L Stainless Steels in Simulated Body Fluids and Cell Cultures," Acta Biomaterialia, vol. 2, no. 6, pp. 709–715, Nov. 2006. https://doi.org/10.1016/j.actbio.2006.06.003

[6] D. J. Young and B. A. Pint, "Chromium Volatilization Rates from Cr_2O_3 Scales into Flowing Gases Containing Water Vapor," Oxidation of Metals, vol. 66, nos. 3–4, pp. 137–153, Oct. 2006. https://doi.org/10.1007/s11085-006-9030-1

[7] D. Jorge-Badiola, A. Iza-Mendia, and I. Gutiérrez, "Evaluation of Intragranular Misorientation Parameters Measured by EBSD in a Hot Worked Austenitic Stainless Steel," Journal of Microscopy, vol. 228, no. 3, pp. 373–383, Dec. 2007. https://doi.org/10.1111/j.1365-2818.2007.01850.x

[8] K. Mino, C. Fukuoka, and H. Yoshizawa, "Evolution of Intragranular Misorientation during Plastic Deformation," Journal of the Japan Institute of Metals, vol. 64, no. 1, pp. 50–55, Jan. 2000. https://doi.org/10.2320/jinstmet1952.64.1_50

[9] N. Attarzadeh, M. Molaei, K. Babaei, et al., "New Promising Ceramic Coatings for Corrosion and Wear Protection of Steels: A Review," Surfaces and Interfaces, vol. 25, p. 100997, Aug. 2021. https://doi.org/10.1016/j.surfin.2021.100997

[10] G. Wang, L. Guo, Y. Ruan, et al., "Improved Wear and Corrosion Resistance of Alumina Alloy by MAO and PECVD," Surface and Coatings Technology, vol. 479, p. 130556, Mar. 2024. https://doi.org/10.1016/j.surfcoat.2024.130556

[11] E. Ozensoy, "Interaction of Water with Ordered θ-Al_2O_3 Ultrathin Films Grown on NiAl(100)," The Journal of Physical Chemistry B, vol. 109, no. 8, pp. 3431–3436, Feb. 2005. https://doi.org/10.1021/jp0449206

[12] G. P. V. Dalmora, E. P. B. Filho, A. A. M. Conterato, et al., "Methods of Corrosion Prevention for Steel in Marine Environments: A Review," Results in Surfaces and Interfaces, vol. 18, p. 100430, Mar. 2025. https://doi.org/10.1016/j.rsurfi.2025.100430

[13] C. Gorle, J. V. Beeck, P. Rambaud, et al., "CFD Modelling of Small Particle Dispersion: The Influence of the Turbulence Kinetic Energy in the Atmospheric Boundary Layer," Atmospheric Environment, vol. 43, no. 3, pp. 673–681, Jan. 2009. https://doi.org/10.1016/j.atmosenv.2008.09.060

[14] S. M. George, "Atomic Layer Deposition: An Overview," Chemical Reviews, vol. 110, no. 1, pp. 111–131, Jan. 2010. https://doi.org/10.1021/cr900056b

[15] M. Liberatore, L. Burtone, T. M. Brown, et al., "On the Effect of Al_2O_3 Blocking Layer on the Performance of Dye Solar Cells with Cobalt Based Electrolytes," Applied Physics Letters, vol. 94, no. 17, p. 173307, Apr. 2009. https://doi.org/10.1063/1.3126051

https://doi.org/10.64486/m.66.1.5

[16] V. E. C. Marques, L. A. Manfroi, A. A. Vieira, et al., "Crystalline structure, morphology, and adherence of thick TiO_2 films grown on 304 and 316L stainless steels by atomic layer deposition," Coatings, vol. 13, no. 4, 2023, https://doi.org/10.3390/coatings13040757

[17] E. Marin, L. Guzman, A. Lanzutti, et al., "Multilayer Al_2O_3/TiO_2 atomic layer deposition coatings for the corrosion protection of stainless steel," Thin Solid Films, vol. 522, pp. 283–288, 2012, https://doi.org/10.1016/j.tsf.2012.08.023

[18] M. Fedel and F. Deflorian, "Electrochemical characterization of atomic layer deposited Al_2O_3 coatings on AISI 316L stainless steel," Electrochim. Acta, vol. 206, pp. 404–415, 2016, https://doi.org/10.1016/j.electacta.2016.02.107

[19] B. Díaz, J. Wiatowska, V. Maurice, et al., "Electrochemical and time-of-flight secondary ion mass spectrometry analysis of ultra-thin metal oxide (Al_2O_3 and Ta_2O_5) coatings deposited by atomic layer deposition on stainless steel," Electrochim. Acta, vol. 56, no. 28, pp. 10516–10523, 2011, https://doi.org/10.1016/j.electacta.2011.02.074

[20] V. H. A. Tran, S. C. Lims, N. Anwar, et al., "Atomic Layer Deposition of Metal and Metal Oxides: Mechanisms, Challenges, and Future Prospects," Journal of Alloys and Compounds, vol. 1041, p. 183864, Sep. 2025. https://doi.org/10.1016/j.jallcom.2025.183864

https://doi.org/10.64486/m.66.1.5